Colloid Polym Sci (2006) 284: 620–626
DOI 10.1007/s00396-005-1408-0

ORIGINAL CONTRIBUTION

J. Fritsch
W. Stille
G. Strobl

Investigation of polymer crystallization kinetics with time dependent light attenuation measurements

Received: 26 August 2005
Accepted: 26 September 2005
Published online: 14 February 2006
© Springer-Verlag 2006

J. Fritsch (✉) · W. Stille · G. Strobl
Physikalisches Institut,
Albert-Ludwigs-Universität,
79104 Freiburg, Germany
e-mail: Jens.Fritsch@emi.fraunhofer.de

Abstract Results obtained for samples of syndiotactic polypropylene and poly(ethylene-co-octene) demonstrated the usefulness of light attenuation measurements in investigations of polymer crystallization. The earlier stages with separated growing spherulites fall in the range of Rayleigh–Debye–Gans scattering. Known relationships describing the dependence of the linear attenuation coefficient on the radius and the index of refraction of a spherulite can be applied in evaluations. The sensitivity of attenuation measurements is much higher than that of conventional tools.

Keywords Polymer crystallization · Light attenuation · Light scattering

Introduction

Investigations of the kinetics of polymer crystallization are usually carried out with the aid of differential scanning calorimetry, X-ray scattering in the wide and small angle range, dilatometry, time dependent vibrational spectroscopy or light scattering experiments. Although based on different properties to derive information about a sample's crystallinity, all these methods end up having a similar sensitivity: reliable data can only be obtained for crystallinities already in the range of several percent of the final value. The end sizes of spherulites are usually in the order of several microns. However, the earliest growing spherulites, which can be detected by these measurements, have already reached the size of several hundred nanometers. This, however, is far from the initial stages of spherulite nucleation and growth.

These early stages have recently gained particular importance in the discussion of the basic mechanisms of polymer crystallization. There are several experimental observations that lead to the assumption of a crystal nucleation and growth, which includes an intermediate phase, although a commonly accepted view did not evolve yet. Some authors propose a preceding coverage of the whole volume by a mesomorphic phase which develops by a mechanism resembling a spinodal process [1, 2] while others point at indications for a nucleation into a mesomorphic phase [3]. Our group favors the view that the mesomorphic phase is right in front of a growing spherulite [4].

Trying to scrutinize these different proposed paths of crystallization we searched for an experimental tool with a sensitivity superior to that of the conventional methods that it can survey crystallization over a larger dynamic range. During the last years we approached this aim by performing time dependent light attenuation measurements investigating a sample's turbidity during crystallization, using the standard set-up of small angle light scattering measurements [5]. Such transmission measurements have the potential for a sensitivity higher than the light scattering experiments, since:

– The decrease in the transmission is due to photons scattered in all directions, whereas the area of the CCD detector is limited.
– It is irrelevant whether a photon is scattered once or several times.

Indeed, we found out that the detectable range of crystallization could be somewhat extended. However, the sensitivity of the technique was limited by the inexact restriction of the integration area, of the employed CCD detector, to a circular region, which is supposed to catch only the primary beam. The technique was also limited by the poor signal-to-noise ratio of the integrated counts and by intensity fluctuations of the laser light source. To

overcome these experimental deficiencies, we developed a novel device that is dedicated to light attenuation measurements. It is based on a comparison of a beam passing through a sample with a reference beam, both being commonly produced by a chopper modulated laser light source, employing lock-in signal detection. The new device yields results with a large increase in sensitivity.

Light attenuation ('turbidity') measurements have already been applied in crystallization studies, but only in a few cases that happened long ago [6–9]. At this time, they were used for qualitative purposes only. By introducing established theoretical relationships for the total cross section for light scattering we have now put the evaluation on a firm basis. In the following we will present our first results which were obtained for crystallizing samples of syndiotactic polypropylene and poly(ethylene-co-octene).

Theoretical background

The attenuation of the light intensity after a passage through a plate-like sample with thickness D is described by the Lambert–Beer law

$$\frac{I}{I_0} = \exp(-\Lambda \mathrm{D}), \tag{1}$$

where I_0 denotes the flux of the light beam at the sample front and I represents the flux remaining after the beam has passed through the sample. The parameter Λ is the linear attenuation coefficient, which can in general be due to scattering and absorption of light. For the polymers under study, the contribution arising from an absorption is negligible for the applied wavelength of λ=635 nm.

The samples used in the experiments were cooled down from temperatures above the equilibrium melting point to a preset crystallization temperature. Changes of the attenuation coefficient during the crystallization process are due to a growth of spherulites or hedrites, both representing centers of light scattering incidents. Their contribution to the linear attenuation coefficient Λ can be expressed by equations. As long as the scattering objects are diluted in the matrix, which is always the case during the initial stages of the crystallization process, Λ is given by

$$\Lambda = \rho\sigma^2, \tag{2}$$

where ρ describes the number density of objects and σ^2 represents the total scattering cross section. σ^2 is usually written as

$$\sigma^2 = \pi R^2 Q. \tag{3}$$

Here, R denotes the radius of the scattering object. Q is called 'scattering efficiency factor'. This scattering efficiency factor is dependent on the size of the scatterer and on the refractive indices of the scatterer, n_s, and surrounding material, n_m. Together they determine the refractive index ratio

$$m = \frac{n_s}{n_m}. \tag{4}$$

A commonly used variable in describing scattering phenomena is the parameter α, defined as

$$\alpha = \frac{2\pi n_m R}{\lambda}, \tag{5}$$

which is proportional to the radius R. Explicit expressions for Q exist only for spherical scatterers isolated in a matrix, and they are given in the literature [10]. Three different ranges for α can be distinguished and are addressed as:

- 'Rayleigh scattering', for α<1
- 'Rayleigh–Debye–Gans scattering' (RDG), for 1<α<$(m-1)^{-1}$
- 'Mie scattering', for α>$(m-1)^{-1}$

As spherulite nucleation starts in the range of some nanometers then proceeds to grow up to several micrometers corresponding to 0.015<α<150, one range would be within the Rayleigh and the Rayleigh–Debye–Gans regime. The scattering efficiency factor in the Rayleigh–Debye–Gans approximation, Q_{RDG}, is given by

$$\begin{aligned} Q_{RDG} = &(m-1)^2\left[\frac{5}{2} + 2\alpha^2 - \frac{\sin(4\alpha)}{4\alpha} - \frac{7}{16\alpha^2}\right. \\ &(1-\cos(4\alpha)) + \left(\frac{1}{2\alpha^2} - 2\right)(0.577 + \ln(4\alpha) \\ &\left. - \mathrm{Ci}(4\alpha))\right], \end{aligned} \tag{6}$$

with

$$\mathrm{Ci}(x) = -\int_x^\infty \frac{\cos x'}{x'} dx'. \tag{7}$$

Equation 6 includes the Rayleigh regime as a limiting case for α<1. An analysis of Eq. 6 reveals for α>1 an approximate proportionality of the scattering efficiency factor Q_{RDG} to the squared radius R^2, thus resulting in a

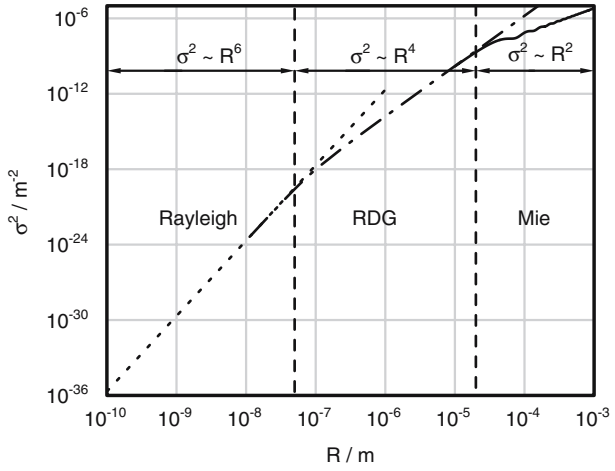

Fig. 1 Scattering cross section σ^2 of spheres with radius R for m=1.0034. Calculations were carried out using: Rayleigh approximation (*dotted line*), RDG approximation (*dash-dotted line*) and Mie approximation (*solid line*)

dependence of the total scattering cross section σ^2 on the object's radius R given by:

$$\sigma^2_{\mathrm{RDG}} \sim (m-1)^2 R^4. \tag{8}$$

The radius dependence of σ^2 over a broader interval of radii can be displayed as done in [5] for the example of low density polyethylene if the calculations for the adjacent Rayleigh and Mie ranges are included. Figure 1 reproduces the results of this calculation. The rather sharp transitions between the three ranges with their different radius dependencies, here located at about 50 nm and 20 μm, are noticeable.

As previously stated, the introduced equations only hold as long as the scattering objects are isolated in the matrix. Application of the equations ends when the objects start touching each other. In fact, the attenuation coefficient passes over a maximum for a coverage of about 50% of the sample with scattering objects, and subsequently decreases until homogeneity is reached when the sample is fully occupied by objects. Light attenuation then still exists due to the varying birefringence within the spherulites. It is caused by variations in the orientation of the optical indicatrix whose direction in the spherulites changes with the orientation of the crystallized chains. The initial dominant scattering caused by the density difference between the melt and the spherulites has disappeared at the end. In qualitative terms, Hawkins and Richards [6] have discussed this time dependence during the later stages. We made no attempt to quantitatively evaluate the kinetics within this part of the measured curves. Our focus was only on the initial stages of polymer crystallization.

Experimental

We carried out the transmission measurements using a chopper modulated two-beam set-up together with lock-in signal detection. The experimental set-up is displayed in Fig. 2. The utilized light source is an intensity stabilized semiconductor laser module manufactured by Global Lasertech, which operated at a wavelength of λ=635 nm with a power of 5 mW. It comprises a built-in monitor photo diode and a processor controlled feedback circuit to suppress intensity fluctuations. After passing through a spacial filter, the laser beam is split into two beams of equal intensity, one passing through the sample – called the

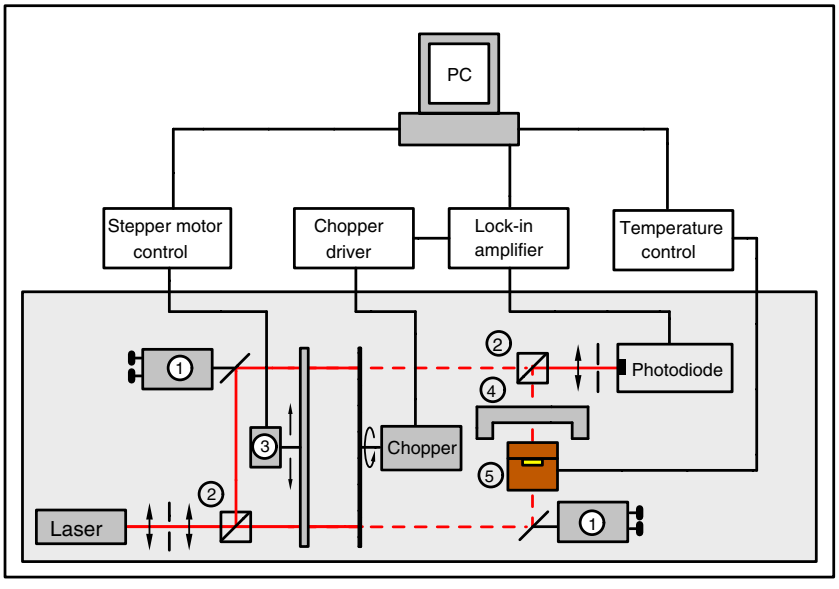

Fig. 2 Experimental set-up for light attenuation measurements. *1*: adjustable mirrors, *2*: beam splitters, *3*: selective beam attenuator, *4*: heat shield, *5*: sample oven

sample beam – while the other is led around the sample, serving as a reference – called the reference beam. The two beams are now directed through a selective beam attenuator – providing at the beginning of the crystallization experiment a precise intensity match of sample and reference beam by attenuating either one or the other – onto a light chopper which alternately transmits only one beam at a time. After passing through the oven containing the sample, the periodically interrupted sample beam is merged again with the opposite phase modulated reference beam by a second beam splitter. The conjunct laser beam is now focused on a pinhole and directed onto a photo diode. This set-up allows the application of a lock-in amplifier for phase-sensitive detection at the chopper frequency, as done in our experiment using a Stanford Research Systems model SR830. The output signal of the lock-in amplifier is proportional to the intensity difference between the sample and reference beam. The data of the time dependent measurements are stored in a PC for further evaluation. Detailed information concerning data acquisition and analysis is included in [11].

The investigated samples chosen according to their final turbidity in the crystalline state were kept between two glass slides and had thickness ranging from 25 up to 500 μm. To achieve high cooling rates so that low temperature isotherms with short crystallization times can be measured, the sample was heated in an external hot stage. Then it was transferred into the sample oven preset at the

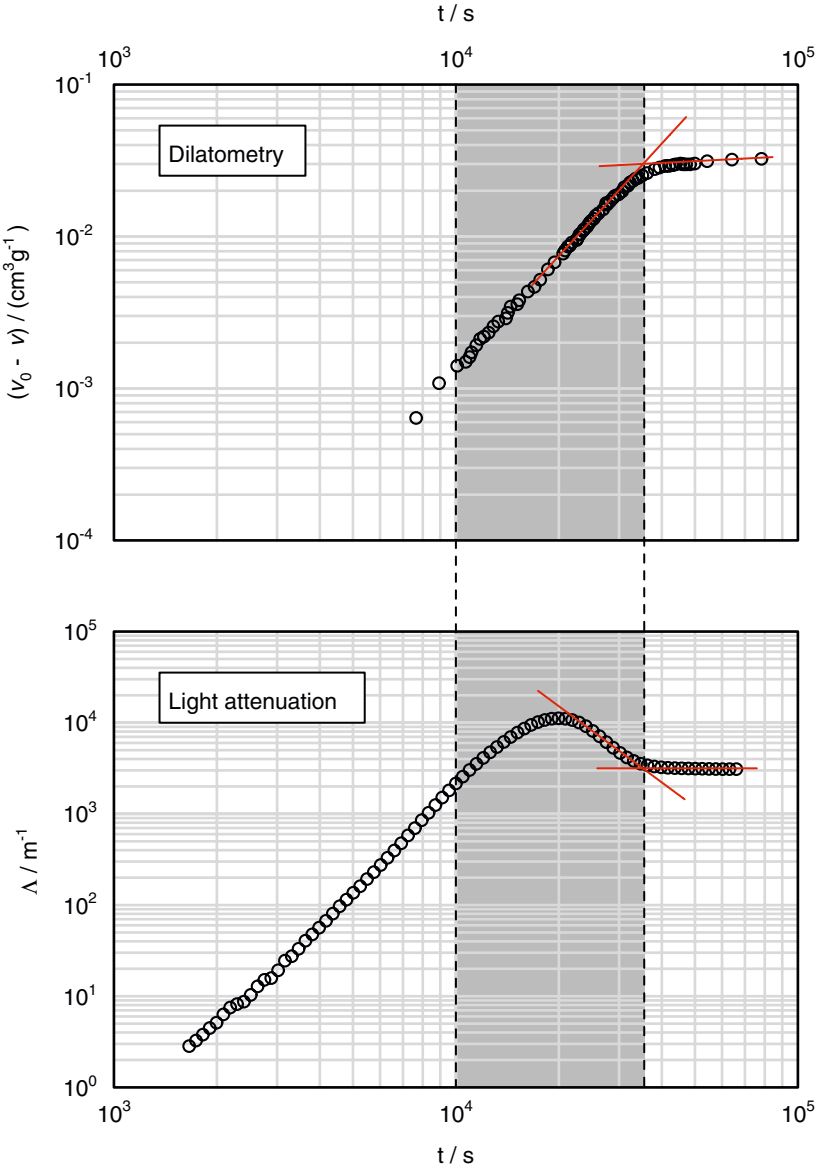

Fig. 3 Comparison of two crystallization isotherms of a sPP sample obtained by a dilatometric and an attenuation measurement for a crystallization temperature of 115°C

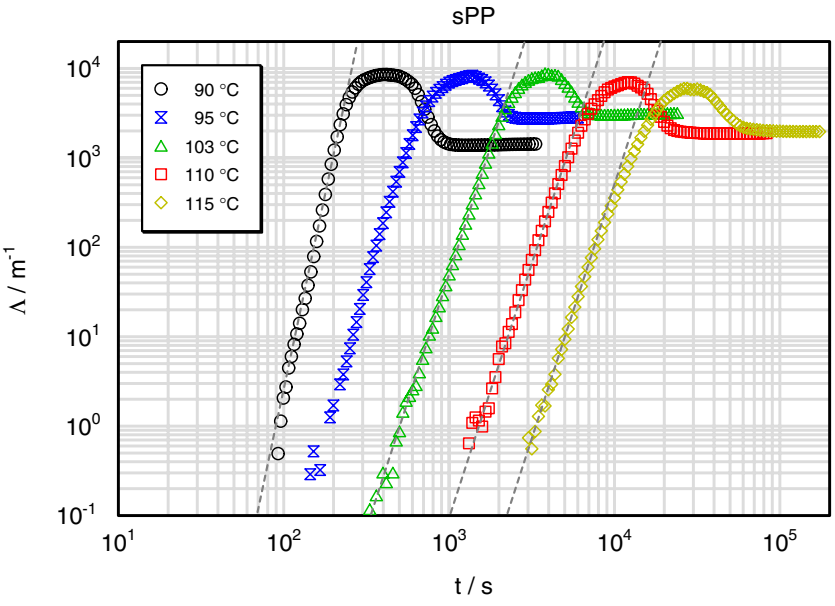

Fig. 4 Crystallization isotherms of a sPP sample in terms of Λ. The sample thickness is 500 μm. The *dashed lines* indicate initial power laws $\Lambda \sim t^5$ and $\Lambda \sim t^8$ for high and low temperatures, respectively

crystallization temperature, reducing the cooling process down to less than 30 s.

The polymers under study were a commercial syndiotactic polypropylene with 83% syndiotactic pentades, sPP, produced by Fina Co., Brussels, and a poly(ethylene-co-octene) of the metallocene catalyst type with an octene weight content of 14%, P(EcO14), supplied by Dow Chemicals Europe.

Results

A crystallization isotherm of sPP measured with the set-up is displayed in Fig. 3 and compared to an isotherm obtained by a dilatometric measurement. The improvement of the sensitivity resulting in an extension of the observable period of crystallization by nearly one order of magnitude is clearly visible.

Figure 4 displays a series of time dependent transmission measurements expressed in terms of Λ, carried out for sPP at different crystallization temperatures. They all exhibit the expected characteristic form: Starting with a constant slope, they reach a maximum for an about 50% volume coverage of the polymer sample by scattering objects, and subsequently decrease as the scatterers grow further until they fill the whole sample. As mentioned, the nonvanishing final value is caused by the varying birefringence of the partially crystalline scattering objects. If the crystallization temperature increases, the measured isotherms are shifted

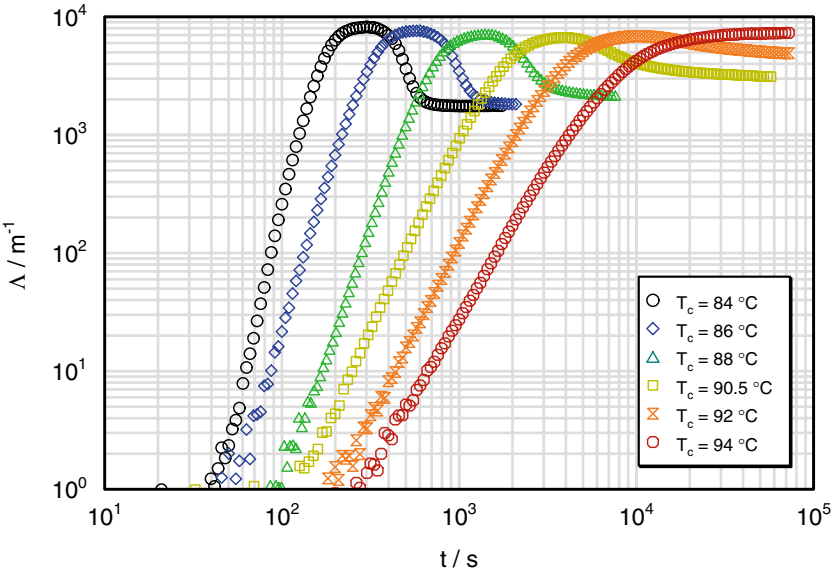

Fig. 5 Crystallization isotherms of a sample of P(EcO14). The sample thickness is 500 μm

toward longer times – approximately one decade every 15 K. In the range of higher crystallization temperatures, we only observed a parallel shift of the isotherms, all having an initial slope of about 5, corresponding to a power law $\Lambda \sim t^5$, as indicated by the dashed line. This slope is constant within each isotherm through three orders of magnitude of the attenuation coefficient Λ, before reaching the maximum related with 50% coverage. In the range of lower crystallization temperatures, an increase in the slope of the isotherms is observed, which reached a value of 8, i.e., indicating $\Lambda \sim t^8$, for a crystallization temperature of 90°C (dash-dotted line).

Figure 5 displays the isotherms measured for a poly (ethylene-co-octene) sample with a thickness of 500 μm. For each isotherm the slope remains constant through nearly four orders of magnitude, until the maximum of Λ is reached. At the highest temperatures, slopes are rather low and then they increase when the crystallization temperature is decreased, from the value of 2 to 6 for the highest (94°C) and lowest (84°C) crystallization temperatures, respectively. Another observation noticed in Fig. 5 is the drop of the maximum value of Λ for increasing crystallization temperatures.

Discussion

The dilatometric crystallization isotherm of sPP in Fig. 3 was taken from a series of measurements reported previously [12]. The slope in the log−log plot indicated for the initial stages of the crystallization process a decrease of the specific volume proportional to t^3 for all crystallization temperatures. Such a behavior is expected if the growing objects – hedrites or spherulites – increase in size with a constant growth rate, i.e., for

$$R \sim t. \tag{9}$$

Therefore, the time dependence of the linear attenuation coefficient Λ in the power law range is expected to be

$$\Lambda \sim R^4 \sim t^4. \tag{10}$$

This is indeed found for Λ within the time and crystallization temperature range of the dilatometric measurements. However, the initial slope, i.e., the one observed in the preceding time range which could not be accessed by dilatometry, is higher, amounting to a value of about 5. Here, an additional contribution to the scattering efficiency exists and it could arise from a change in the inner crystallinity of the scatterers. This would lead to a change in the refractive index ratio m and hence to a change of the attenuation coefficient according to the relationship $\Lambda \sim (m-1)^2$. With Eq. 4, and taking into account that

$$n_S = (1 - \phi_{c,i}) n_m + \phi_{c,i} n_c \tag{11}$$

with n_c representing the refractive index of crystallites, we can obtain

$$\Lambda \sim \phi_{c,i}^2, \tag{12}$$

where $\phi_{c,i}$ represents the inner crystallinity of the scattering objects. The measured slope of 5, obtained for the sPP sample when crystallized at high temperatures, can therefore be understood as resulting from two factors, namely a growth of a spherulite and the simultaneous increase of the inner crystallinity.

The mechanism that leads to the initial power law $\Lambda \sim t^8$ observed for the lowest crystallization temperature is not yet understood. It would be interesting to compare these results with other experiments. Conventional tools cannot enter this domain of short crystallization times, but modern calorimetric techniques would allow it since they can register even more rapid crystallization processes [13].

The investigated poly(ethylene-co-octene) sample exhibits crystallization isotherms with log−log plot slopes varying from approximately 2 to 6 — again the slope increases when the crystallization temperature decreases. According to Eq. 12, isotherms with a slope of 2, as they are measured for the highest crystallization temperature, have to be interpreted as resulting from a first order in-filling process of crystallites into objects of virtually constant size. This increase of the inner crystallinity can be observed over two orders of magnitude, corresponding to four orders of magnitude in Λ. On the other hand, the creation of the objects that become filled by the crystallites is not detected. The same kinetics of in-filling had already been observed in the investigations of P(EcO14) with a polarizing optical microscope [14]. Here, a diffuse 'precursor' structure with length scales in the micrometer range already showed up at the beginning of the structural observations and then increased in visibility. The observation also indicated an increase in the inner crystallinity of given objects without changes in their geometry. The fact that the creation of the precursor structure is still not detected when using the much more sensitive attenuation measurements means that the density difference against the melt of these objects in the initial, empty state, $\Delta\rho_{in}$ is indeed extremely low. As we follow the filling process over two orders of magnitude, $\Delta\rho_{in}$ must be below 10^{-4} g cm^{-3} (the completely filled objects show a density difference $\Delta\rho \approx 10^{-2}$ g cm^{-3} corresponding to an inner crystallinity of about 10%). When the objects are filled they show the

birefringence pattern of spherulites. We speculate that the objects in the initial state are made of a few dominant crystalline lamellae which grew rapidly in advance, prior to the large majority of lamellar crystallites.

Acknowledgements We highly appreciate the advice given by Georg Maret (University Konstanz). We also gratefully acknowledge the funding given by the Deutsche Forschungsgemeinschaft. Thanks are also due to the 'Fonds der Chemischen Industrie' for the financial support.

References

1. Imai M, Kaji K, Kanaya T, Sakai Y (1995) Phys Rev B 52:12696
2. Olmsted PD, Poon WCK, McLeish TCB, Terrill TCB, Ryan AJ (1998) Phys Rev Lett 81:373–376
3. Kraak H, Deutsch M, Sirota EB (2000) Macromolecules 33:6174
4. Strobl G (2000) Eur Phys J, E 3:165
5. Heck B, Kawai T, Strobl G (2006) Polymer (in press)
6. Hawkins SW, Richards RB (1949) J Polym Sci 4:515
7. Keane JJ, Stein RS (1956) J Polym Sci 20:327
8. Levy B (1961) J Appl Polym Sci 5:408
9. Mahen KG, James WJ, Bosch W (1965) J Appl Polym Sci 9:3605
10. Kerker M (1969) The scattering of light. Academic Press, p 418
11. Fritsch J (2005) Diplomarbeit, Physikalisches Institut, Universität Freiburg
12. Heck B, Strobl G (2004) Colloid Polym Sci 282:5117
13. Adamovsky S, Schick Ch (2004) Thermochim Acta 415:1
14. Häfele A, Heck B, Kawai T, Kohn P, Strobl G (2005) Eur Phys J E Soft Matter 16:207